DALTON
FULL PAPER

Complexes containing redox-active fluorenone-based ligands linked to redox-active tris(pyrazolyl)boratomolybdenum fragments: assignment of ligand-centred and metal-centred redox processes by EPR and UV/VIS/NIR spectroelectrochemistry †

Andreas Behrendt, Samantha M. Couchman, John C. Jeffery, Jon A. McCleverty * and Michael D. Ward *

School of Chemistry, University of Bristol, Cantock's Close, Bristol, UK BS8 1TS.
E-mail: mike.ward@bristol.ac.uk, jon.mccleverty@bristol.ac.uk

Received 9th September 1999, Accepted 9th November 1999

The dinuclear complex [{Mo($Tp^{Me,Me}$)(NO)Cl}$_2$(μ-L^2)] **2** [L^2 is the new bridging ligand 2,7-bis{2-(4-pyridyl)ethen-1-yl}fluorenone] contains two redox-active molybdenum(I) centres linked by a bridging ligand which is itself redox-active by virtue of the fluorenone spacer unit. The complex undergoes four one-electron reductions of which two are metal-centred Mo(0)/Mo(I) couples and two are reductions of the fluorenone unit. Also studied were the mononuclear analogue [Mo($Tp^{Me,Me}$)(NO)Cl(L^1)] [L^1 is 2-bromo-7-{2-(4-pyridyl)ethen-1-yl}fluorenone], and the dinuclear complex [{Mo($Tp^{Me,Me}$)(NO)Cl}$_2$(μ-L^3)] **3** [L^3 is the bridging ligand 2,7-bis{2-(4-pyridyl)ethen-1-yl}fluorene] which lacks the ligand-centred redox activity. A combination of EPR and UV/VIS/NIR spectroelectrochemical techniques was used and showed how the separate metal-centred and ligand-centred reduction processes lead to quite distinct and characteristic spectroscopic signatures, such that it was possible to assign the sequence of reduction sites as ligand–metal–metal–ligand. The initial reduction of the bridging ligand in **2** results in a much larger separation between the two Mo(0)/Mo(I) couples (240 mV) than occurs in complexes where the bridging ligand is not redox-active.

We have been investigating how metal–metal interactions (both magnetic and electronic) in polynuclear complexes are influenced by the nature of the bridging ligand which links the metal centres and which provides the pathway through which the interactions are transmitted.[1–4] The development of bridging ligands which can mediate long-distance electronic interactions between metal centres is of interest for the development of 'molecular wires',[5] inasmuch as electronic delocalisation in dinuclear complexes can be said to resemble bulk electron flow in a microscopic circuit. Optimisation of magnetic exchange interactions between adjacent metal centres according to the nature of the bridging ligand between them is of interest for the design of materials displaying useful bulk magnetic properties.[6] More immediately, the study of ligand-bridged dinuclear complexes continues to be a popular academic exercise in its own right because of the insight such complexes afford into the fundamental phenomena of metal–metal interactions in environments where the metal–metal separation, and the pathway between them, can be precisely controlled.[7]

In this paper we describe the syntheses, electrochemical and spectroscopic properties of a dinuclear complex in which two redox-active Mo–$Tp^{Me,Me}$ units [$Tp^{Me,Me}$ is hydrotris(3,5-dimethylpyrazolyl)borate] are linked by a conjugated bridging ligand containing a fluorenone unit which is itself redox-active, such that we have the possibility of both metal-centred and ligand-centred redox processes. A combination of UV/VIS/NIR and EPR spectroelectrochemical studies, on the dinuclear complex as well as appropriate model compounds, have allowed assignment of the redox processes. In addition some of the complexes display intense, redox-switchable absorbance in the near-IR region of the electronic spectrum which makes them of interest as electrochromic dyes.[3,8–10]

† *Supplementary data available*: rotatable 3-D crystal structure diagram in CHIME format. See http://www.rsc.org/suppdata/dt/1999/4349/

Experimental

2,7-Dibromo-9-fluorenone, 2,7-dibromofluorene and 4-vinylpyridine were obtained from Aldrich and used as received. [Mo($Tp^{Me,Me}$)(NO)Cl_2] was prepared according to the published method.[11]

Instrumentation used for standard spectroscopic measurements, cyclic voltammetry and UV/VIS/NIR spectroelectrochemical measurements has been described previously.[12] The EPR spectroelectrochemical experiments were performed using a cell built according to a published design[13] in a Bruker ESP-300E spectrometer at room temperature. ZINDO calculations were performed using a CAChe workstation using INDO/1 parameters and a configuration interaction level of 15 to calculate the electronic spectra.[14] All electrochemical measurements were made using purified thf or CH_2Cl_2 as solvent at room temperature. Spectroelectrochemical studies were carried out in thf or CH_2Cl_2 at −30 °C, and the chemical reversibility of all processes was confirmed by reversing the applied potential and regenerating the spectrum of the starting material.

Preparations

Ligand L^1. A mixture of 2,7-dibromo-9-fluorenone (2.00 g, 5.92 mmol), 4-vinylpyridine (3.0 cm^3, 2.93 g, 2.78 mmol), palladium(II) acetate (0.055 g, 0.24 mmol) and triphenylphosphine (0.100 g, 0.38 mmol) in dry triethylamine (40 cm^3) was heated to reflux under N_2 for 24 h, during which time an orange precipitate appeared. After removal of the solvent *in vacuo*, the precipitate was collected by filtration, washed with water and then small portions of dichloromethane, and dried. Yield: 1.3 g (60%). EIMS: *m*/*z* 361, 363 (100% each, M^+; two peaks arising from ^{79}Br and ^{81}Br isotopes). Found: C, 66.0; H, 3.1; N, 3.7%. $C_{20}H_{12}NOBr$ requires: C, 66.3; H, 3.3; N, 3.9%.

Ligand L^2. A mixture of L^1 (1.00 g, 2.76 mmol), 4-vinyl-

pyridine (3.0 cm^3, 2.93 g, 2.78 mmol), palladium(II) acetate (0.055 g, 0.24 mmol) and triphenylphosphine (0.100 g, 0.38 mmol) in dry triethylamine (40 cm^3) was heated to reflux under N_2 for 5 days. The precipitate was collected by filtration, washed with copious amounts of water and then CH_2Cl_2, and dried. The material prepared in this way is sufficiently pure for further use. Yield: 0.40 g (37%). EIMS: *m*/*z* 386 (100%, M^+). Found: C, 83.1; H, 4.3; N, 7.5%. $C_{27}H_{18}N_2O$ requires: C, 83.9; H, 4.7; N, 7.3%.

Ligand L^3. A mixture of 2,7-dibromofluorene (1.50 g, 4.63 mmol), 4-vinylpyridine (1.54 cm^3, 1.50 g, 14.2 mmol), triethylamine (5 cm^3), palladium(II) acetate (0.034 g, 0.15 mmol) and triphenylphosphine (0.079 g, 0.30 mmol) was sealed in a Schlenk tube under nitrogen and heated to 100 °C, with stirring, until a solid mass had formed (*ca.* 2 days). The solid product was suspended in dichloromethane (100 cm^3) and shaken vigorously with water (200 cm^3) in a separating funnel. The organic layer was collected, dried ($MgSO_4$) and evaporated to dryness to give pure L^3. Yield: 0.64 g (37%). EIMS: *m*/*z* 372 (100%, M^+). Found: C, 86.5; H, 5.0; N, 7.1%. $C_{27}H_{20}N_2$ requires: C, 87.1; H, 5.4; N, 7.5%.

[Mo($Tp^{Me,Me}$)(NO)Cl(L^1)] 1. A mixture of L^1 (0.150 g, 0.41 mmol), [Mo($Tp^{Me,Me}$)(NO)Cl_2] (0.202 g, 0.41 mmol) and dry Et_3N (0.5 cm^3) in dry toluene (30 cm^3) was heated to reflux for 12 h. After cooling the solvent was removed *in vacuo*, and the residue was purified by column chromatography on silica eluting initially with CH_2Cl_2. After removal of a fast-eluting pale green material, the product was eluted as a red-brown band using CH_2Cl_2–thf (96:4). The combined fractions containing the product were concentrated to a volume of *ca.* 5 cm^3, and addition of hexane then precipitated the product which was filtered off and dried. Yield: 0.185 g (54%). FABMS: *m*/*z* 821 (M^+, 100%); 784 ($M^+ - Cl$, 20%). Found: C, 51.3; H, 3.9; N, 13.1%. $C_{35}H_{34}BBrClMoN_8O_2$ requires: C, 51.1; H, 4.1; N, 13.6%.

[{Mo($Tp^{Me,Me}$)(NO)Cl}$_2$(μ-L^2)] 2. This was prepared in the same way as **1**, from L^2 (0.185 g, 0.48 mmol), [Mo($Tp^{Me,Me}$)(NO)Cl_2] (0.500 g, 1.01 mmol) and dry Et_3N (0.5 cm^3) in dry toluene (50 cm^3) at reflux for 12 h. Column chromatography on silica using CH_2Cl_2–thf (98:2) as eluent afforded pure **2**. Yield: 0.276 g (44%). FABMS: *m*/*z* 1303 (M^+, 10%), 1268 ($M^+ - Cl$, 2%), 846 ($M^+ - \{Mo(Tp^{Me,Me})(NO)Cl\}$, 70%), 811 ($M^+ - \{Mo(Tp^{Me,Me})(NO)Cl\} - Cl$, 40%). Found: C, 52.6; H, 4.8; N, 16.7%. $C_{57}H_{62}B_2Cl_2Mo_2N_{16}O_3$ requires: C, 52.5; H, 4.8; N, 17.2%.

[{Mo($Tp^{Me,Me}$)(NO)Cl}$_2$(μ-L^3)] 3. A mixture of L^3 (0.200 g, 0.538 mmol), [Mo($Tp^{Me,Me}$)(NO)Cl_2] (0.800 g, 1.61 mmol) and dry triethylamine (2 cm^3) in dry toluene (60 cm^3) was stirred and refluxed under nitrogen for 24 h. Workup as above followed by column chromatography on silica using CH_2Cl_2–thf (98:2) as eluent afforded pure **3** as a very dark microcrystalline powder. Yield: 0.25 g (41%). FABMS: *m*/*z* 1289 (M^+, 15%), 1245 ($M^+ - Cl$, 5%). Found: C, 53.3; H, 5.0; N, 16.8%. $C_{57}H_{64}B_2Cl_2Mo_2N_{16}O_2$ requires: C, 53.1; H, 5.0; N, 17.4%.

X-Ray crystallography

Crystal data for complex **2**·5.5CH_2Cl_2: $C_{62.5}H_{73}B_2Cl_{13}Mo_2N_{16}O_3$, $M = 1770.72$, triclinic, space group $P\bar{1}$, $a = 9.401(2)$, $b = 17.730(4)$, $c = 25.841(7)$ Å, $\alpha = 105.48(2)$, $\beta = 93.23(2)$, $\gamma = 100.63(2)°$, $V = 4054(2)$ Å^3, $T = 173$ K, $Z = 2$, μ(Mo-Kα) = 0.789 mm^{-1}. 27335 reflections were measured with $2\theta_{max} = 45°$, which after merging afforded 10527 unique data ($R_{int} = 0.158$). All data were used in subsequent calculations. Final $wR2 = 0.320$; $R1 = 0.105$. The instrument used was a Siemens SMART-CCD diffractometer. Software used: SHELXS-97 for structure solution;[15] SHELXL-97 for structure refinement;[15] SADABS for the absorption correction.[16]

Crystals of **2**·5.5CH_2Cl_2 were fragile and lost solvent easily; despite rapid mounting of the crystal at 173 K some decomposition occurred. In addition two of the CH_2Cl_2 solvent molecules have their Cl atoms disordered over two sites, and one of the CH_2Cl_2 molecules only refined satisfactorily with site occupancies of 50% for all of its atoms. Restraints were applied to the geometric and thermal parameters of these solvent molecules to allow them to refine stably. The combination of solvent loss and disorder of relatively heavy Cl atoms resulted in very weak data which accounts for the rather poor quality of the refinement ($R1 = 10.5\%$). Although the overall structure of the molecule is perfectly clear, we prefer not to comment in detail on bond lengths and angles (a table of such data is therefore not included) except to note that the coordination geometry around the metal centres is about the same as we have observed in other complexes of this general type (see Results and discussion section).

CCDC reference number 186/1727.

See http://www.rsc.org/suppdata/dt/1999/4349/ for crystallographic files in .cif format.

Results and discussion

Syntheses of ligands and complexes, and the crystal structure of complex 2

The new ligands (see Chart 1) were prepared by a standard

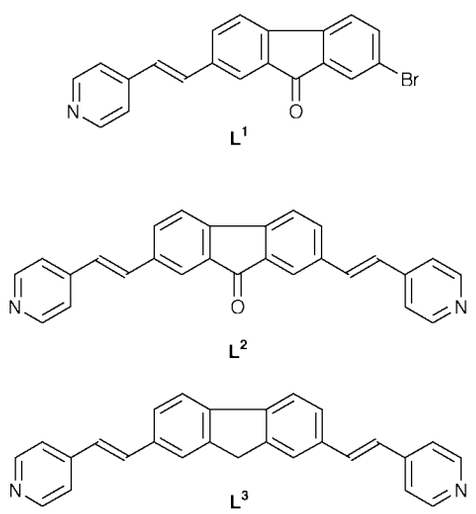

Chart 1

Heck coupling of 4-vinylpyridine with 2,7-dibromo-9-fluorenone (for L^1 and L^2) or 2,7-dibromofluorene (for L^3), a method we have used extensively for preparing related bridging ligands.[17] For L^1 and L^2 the reaction could be controlled by its stepwise nature: reaction of 2,7-dibromo-9-fluorenone with only half an equivalent of 4-vinylpyridine ensured a reasonable yield of L^1, and reaction of L^1 with further 4-vinylpyridine under forcing conditions afforded L^2. The ligands were characterised on the basis of their mass spectra and elemental analyses; their very poor solubility precluded characterisation by ^{1}H NMR spectroscopy. The significance of L^3 is that in the absence of the carbonyl group compared to L^2, *i.e.* conversion of a fluorenone unit to fluorene, the ligand-centred redox activity is lost.

Reaction of L^1–L^3 with the diamagnetic 16-electron complex [Mo($Tp^{Me,Me}$)(NO)Cl_2] afforded complexes [Mo($Tp^{Me,Me}$)(NO)Cl(L^1)] **1**, [{Mo($Tp^{Me,Me}$)(NO)Cl}$_2$(μ-L^2)] **2** and [{Mo($Tp^{Me,Me}$)(NO)Cl}$_2$(μ-L^3)] **3** in the usual way,[4,17] by displacement of one chloride ligand by an incoming pyridyl ligand and a concomitant one-electron reduction of the metal centre to

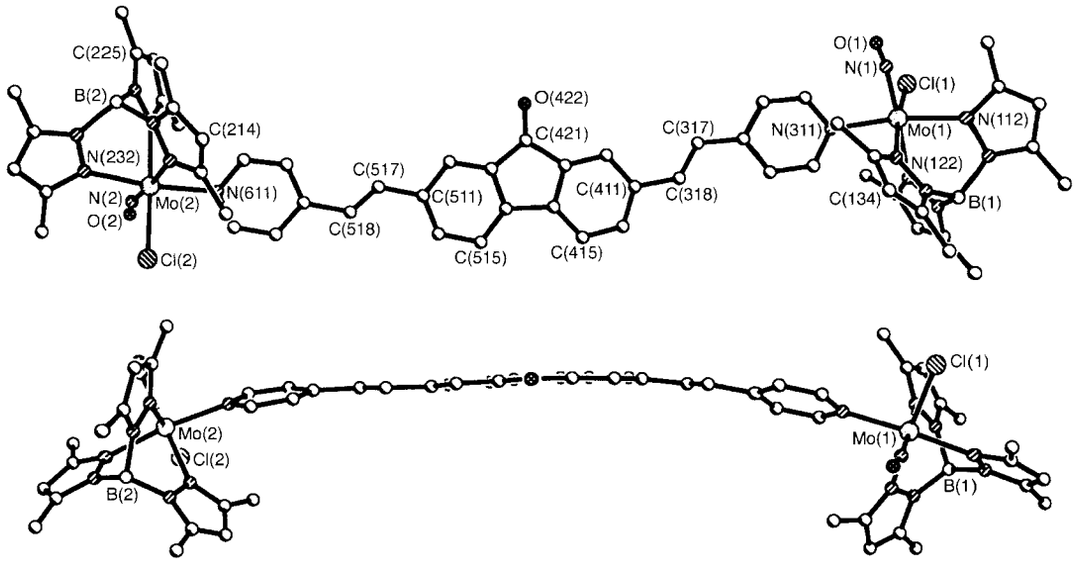

Fig. 1 Two views of the crystal structure of **2**·5.5CH_2Cl_2.

give a paramagnetic 17-electron [formally Mo(I)] configuration. The identity of all complexes was confirmed by satisfactory elemental analyses and FAB mass spectra, as well as by their subsequent electrochemical and spectroscopic behaviour.

X-Ray quality crystals of **2**·5.5CH_2Cl_2 were grown from CH_2Cl_2–hexane, and the crystal structure is shown in Fig. 1. The quality of the refinement is modest ($R1 = 10.5\%$) due to a combination of poor crystallinity and a substantial number of disordered CH_2Cl_2 molecules, both of which resulted in the diffracted data being very weak, but the overall structure is clear and the bond lengths and angles around the metal centres are in agreement with those determined from other (better quality) structural determinations.[8] The important point to note is the overall shape of the molecule, with a very elongated shape (the Mo···Mo separation is 23.97 Å) and the highly conjugated bridging ligand being near-planar apart from a slight degree of curvature.

Electrochemical properties of the complexes

It is well established that mononuclear complexes of the type [$Mo(Tp^{Me,Me})$(NO)Cl(py)], where py is a pyridine derivative or related ligand, undergo chemically reversible one-electron Mo(I)/Mo(II) and Mo(0)/Mo(I) couples, *i.e.* the mononuclear unit can be both oxidised and reduced.[8,17,18] In general the oxidation to Mo(II) occurs at a potential which is not sensitive to the presence of substituents on the pyridine ligand, suggesting that the oxidation is in a substantially metal-centred orbital; in contrast the potential for reduction to Mo(0) is strongly sensitive to the nature of the ligand substituents on the pyridine ligand, suggesting that the electron is added into an orbital which is more delocalised over the metal ion and the pyridine ligand. A consequence of this is that in dinuclear complexes with a conjugated bridging ligand, the two Mo(I)/Mo(II) couples are generally coincident, whereas the two Mo(0)/Mo(I) couples are substantially split due to delocalisation across the bridging ligand in the reduced mixed-valence state.[1,18] Thus, although we describe these processes as 'Mo(0)/Mo(I) couples', it should be borne in mind that they may have significant pyridine-centred character.

The cyclic voltammograms of **1**–**3** are collected in Fig. 2. All of the redox processes depicted are chemically reversible (as shown by spectroelectrochemistry, see later) but have peak–peak separations in the range 100–200 mV indicating possible contributions from (i) slightly slow electron-transfer kinetics, (ii) uncompensated resistance from the solvent, and (iii) unresolved separation of two closely-spaced one-electron waves

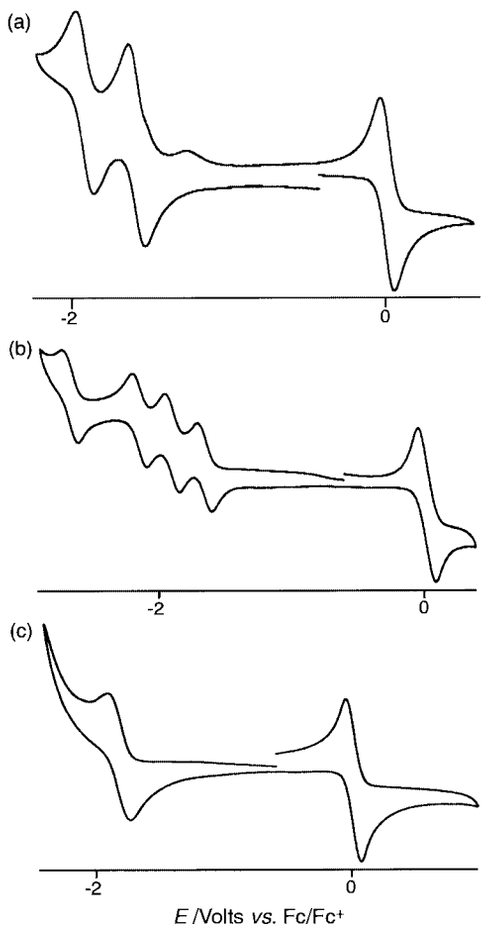

Fig. 2 Cyclic voltammograms of (a) **1**, (b) **2** and (c) **3**.

in the dinuclear complexes. This is entirely typical behaviour for [$Mo(Tp^{Me,Me})$(NO)Cl(py)] units.[8,17,18]

The behaviour of complex **3** will be discussed first as it is the simplest. The voltammogram shows two symmetric waves centred at +0.02 and −1.80 V *vs.* Fc/Fc^+. Each of these corresponds to two synchronous one-electron processes; thus the two Mo(I)/Mo(II) couples occur together at +0.02 V, and the two Mo(0)/Mo(I) couples occur together at −1.80 V. No electrochemical interactions (which would be apparent as splittings of these into two successive one-electron processes) are discernible, although the reduction wave is noticeably broad ($\Delta E_p = 200$

mV), consistent with unresolved slight splitting of the two one-electron waves. This voltammogram is unremarkable and entirely typical of the behaviour shown by other dinuclear complexes of this type in which the electrochemical interaction is too small to detect.[4,17]

The cyclic voltammogram of complex **1** in CH_2Cl_2 shows three one-electron redox processes, of which two may be assigned to the expected metal-based redox processes as described above, whereas the third is assigned to reduction of the redox-active fluorenone unit on the ligand. It is clear that the process at +0.02 V *vs.* Fc/Fc^+ is the Mo(I)/Mo(II) couple, but of the remaining two processes at −1.68 and −2.01 V *vs.* Fc/Fc^+ it is not obvious which is the metal-based Mo(0)/Mo(I) couple, and which is the reduction of the fluorenone unit to its radical anion. Typically, complexes containing [Mo($Tp^{Me,Me}$)(NO)Cl(py)] units with a conjugated substituent on the pyridine ligand undergo reduction between −1.6 and −1.9 V *vs.* Fc/Fc^+,[7,17,18] (*cf.* complex **3** above), and fluorenones reduce in the same region at potentials whose exact value depends on the substituents attached to the fluorenone core.[19] Whichever site is reducing first makes the second site more difficult to reduce *via* the usual electrostatic interaction, which accounts for the rather negative potential of the second process. The natures of these reduction processes were assigned through spectroelectrochemical experiments (see later).

The voltammogram of dinuclear complex **2** in thf is considerably more complicated, showing five redox processes (in CH_2Cl_2 the most negative of these lies outside the solvent/base electrolyte window, which is why we used thf in this case). Of these the process at most positive potential (at +0.02 V *vs.* Fc/Fc^+) is twice the intensity of the others and corresponds to simultaneous oxidation of both metal centres, as in complex **3**.[4,17,18] The four reductions, at −1.66, −1.90, −2.14 and −2.65 V *vs.* Fc/Fc^+ therefore correspond to two distinct one-electron metal-centred processes [Mo(0)/Mo(I) couples] and two distinct one-electron reductions of the disubstituted fluorenone bridging ligand.[19] As with complex **1**, spectroelectrochemical methods are required to assign these more fully.

EPR spectroelectrochemistry of complex 1

Reduction of **1** to $[\mathbf{1}]^-$ by *in situ* electrolysis in an EPR tube resulted in the sequence of spectra shown in Fig. 3. Initially [Fig. 3(a)], the spectrum is entirely typical of mononuclear 17-electron [Mo($Tp^{Me,Me}$)(NO)Cl(py)] complexes,[1,4,17,18] with a central singlet ($g = 1.978$) arising from the *ca.* 75% of Mo isotopes with no nuclear spin, and the superimposed sextet ($A = 50$ G) arising from the remaining *ca.* 25% of Mo isotopes which have $I = 5/2$.

On reduction of this to $[\mathbf{1}]^-$ the spectra could evolve in one of two ways, depending on whether the reduction is metal- or ligand-centred. Metal-centred reduction would give a diamagnetic, 18-electron Mo(0) complex and in this case we would expect the EPR signal of **1** to slowly disappear as the reduction proceeds. Reduction of the fluorenone group in contrast would give a diradical [17-electron Mo(I) centre, and a fluorenone radical anion], and this appears to be the case here. Successive spectra recorded as the reduction proceeds [Fig. 3(b) and 3(c)] show that the initial signal at $g = 1.978$ (labelled with an arrow) slowly disappears, and is replaced by a new signal (labelled with a *) which grows in intensity at $g = 1.990$. This new signal is at a position exactly intermediate between those expected from the Mo-centred radical ($g = 1.978$) and a ligand-centred radical (typically $g = 2.002$), indicating that it arises from magnetic exchange between the two unpaired electrons and the g-value is averaged. We have observed before in other asymmetric diradicals how a single signal at a g-value average for the two sites occurs when the unpaired electrons are exchange-coupled.[20] We were unable to drive this electrolysis to completion in the EPR cell—a weak signal at $g = 1.978$ from a trace of unreacted **1** persisted even after prolonged electrolysis, see Fig. 3(c)—which precludes any analysis of the hyperfine components of the signal. However it is clear from this experiment the first reduction of **1** is ligand-centred, involving reduction of the fluorenone unit to its radical anion, and therefore that the second reduction must be the metal-based Mo(I)/Mo(0) process.

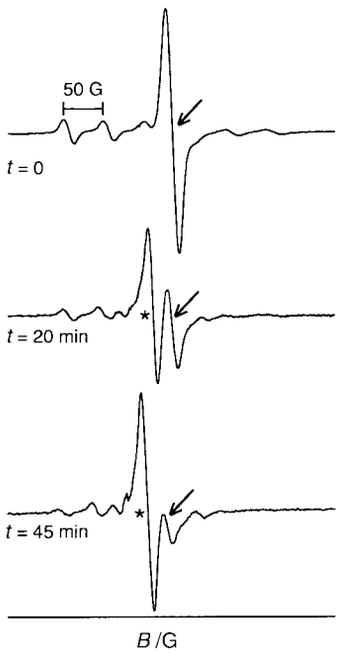

Fig. 3 EPR spectra recorded during reduction of **1** to $[\mathbf{1}]^-$, showing the collapse of the signal at $g = 1.978$ (arrow) and the appearance of a new signal at 1.990 (*).

UV/VIS/NIR spectroelectrochemistry of model compounds: spectroscopic consequences of metal-based and ligand-based reductions

Having assigned the reductions of **1** unambiguously by EPR spectroscopy we can now relate the sites of the reductions to the electronic spectra of the complex in its different oxidation states. To assist in this it is helpful to know the spectroelectrochemical behaviour of the component parts, *i.e.* the [Mo($Tp^{Me,Me}$)(NO)Cl(py)] complex unit and the fluorenone unit.

We described recently the necessary spectroelectrochemical studies on mononuclear [Mo($Tp^{Me,Me}$)(NO)Cl(py)] complexes containing a variety of substituted pyridine derivatives (py) as ligands,[8] and also on dinuclear analogues [{Mo($Tp^{Me,Me}$)(NO)Cl}$_2$(μ-L)] where L is an extended bis(4-pyridyl)polyene bridging ligand.[4] In the parent 17-electron state the lowest-energy features in the electronic spectra of these complexes are Mo(I)→py(π*) MLCT transitions, which occur in the region 450–650 nm and have moderate intensity (ε 1000–5000 dm^3 mol^{-1} cm^{-1}). On reduction to the 18-electron [Mo(0)] state an intense new low-energy transition appears which is a Mo(0)→py(π*) transition. Compared to the MLCT transition in the Mo(I) complex, the new transition is red-shifted because the metal frontier orbital is raised in energy on reduction, and is of much greater intensity because the metal centre is more electron-rich and therefore a better π-donor. If the pyridine derivative is of low symmetry such that it has several low-lying π* levels then two or more MLCT transitions may be visible.[8] In mononuclear [Mo($Tp^{Me,Me}$)(NO)Cl(py-R)]$^-$ for example (py-R = 4-nonylpyridine) the Mo(0)→py MLCT occurs at 830 nm ($\varepsilon = 12000$ dm^3 mol^{-1} cm^{-1}),[7] and in the extended dinuclear complex [{Mo($Tp^{Me,Me}$)(NO)Cl}$_2${NC_5H_4-$(CH{=}CH)_4C_5H_4N$}]$^-$ it occurs at 1282 nm ($\varepsilon = 65000$ dm^3 mol^{-1} cm^{-1}).[4] Metal-based reduction of **1** and **2** should therefore be spectroscopically obvious.

Table 1 Electronic spectra of fluorenone (**Fl**) and its electrochemically-generated radical anion (**Fl**$^{\bullet -}$)

		λ_{max}/nm (10^{-3} ε/dm^3 mol^{-1} cm^{-1})						
Fl	Observed[a]	258 (86)	295 (3.7)	378 (0.27)				
	Calculated[b]	259 (100)	300 (sh)	452 (2)				
Fl$^{\bullet -}$	Observed[a]	269 (30)	287 (59)	351 (0.93)	468 (0.61)[c]	535 (0.98)[c]	717 (0.065)	775 (sh)
	Calculated[b]	261 (60)	293 (28)	366 (5.5)	465 (5.0)		696 (2.0)	

[a] Measured at 243 K in CH_2Cl_2 containing 0.2 M $N^nBu_4PF_6$. [b] Calculated using the ZINDO method; see text. [c] These two peaks may be part of a monomer–dimer equilibrium (see ref. 20); only one peak is predicted by the ZINDO method in this area in the spectrum of the pure monomer radical anion.

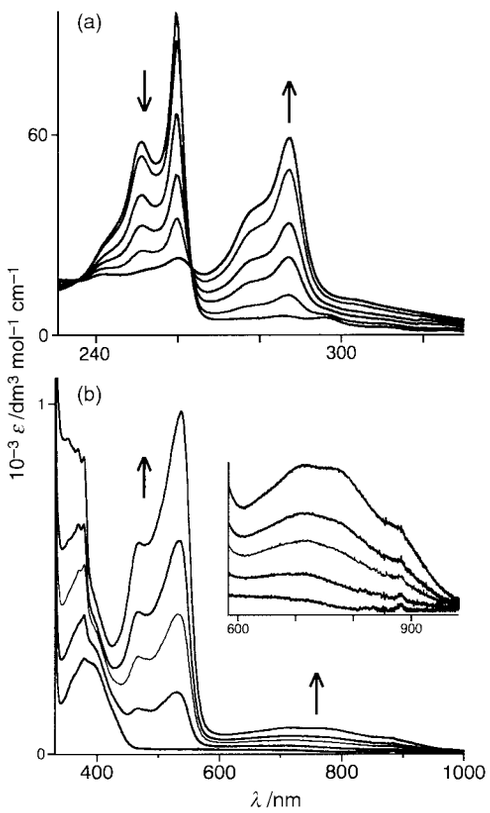

Fig. 4 Electronic spectra recorded during reduction of fluorenone to its radical anion.

The electronic spectrum of fluorenone (hereafter abbreviated **Fl**) is well understood, with three π→π* transitions centred at *ca.* 260, 300 and 380 nm, of which the first two show fine structure due to vibrational progressions.[21] The ketyl radical anion of fluorenone (hereafter abbreviated **Fl**$^{\bullet -}$) has a strong absorbance at *ca.* 500 nm whose exact position and shape are strongly dependent on concentration, solvent, and the nature of the counter-ion because of a monomer–dimer equilibrium.[22] However beyond this little is known: these reports are relatively old with the spectra being studied over a narrow range. For this reason we have carried out a spectroelectrochemical study of reduction of fluorenone; the results are in Fig. 4 (see also Table 1).

On reduction of **Fl** to **Fl**$^{\bullet -}$, the highest-energy π→π* transition of **Fl** at 259 nm collapses, whereas the much less intense π→π* transition of **Fl** at 295 nm (several vibrational components are visible) correspondingly gains in intensity [Fig. 4(a)]. The weak, lowest-energy π→π* transition of **Fl** at 380 nm increases in intensity, and a new transition grows in the visible region at 536 nm with a high-energy shoulder at 468 nm [Fig. 4(b)]. This new transition is the one which has been discussed in the early literature, and the presence of two components may arise from the monomer–dimer equilibrium mentioned earlier.[22] Also present in the spectrum of **Fl**$^{\bullet -}$ is a weak transition at 717 nm ($\varepsilon = 65$ dm^3 mol^{-1} cm^{-1}), with a low-energy shoulder at *ca.* 775 nm, which has not to our knowledge been observed before [see the inset in Fig. 4(b)]. The overall result is a general red-shift of the significant spectral features, with the intense absorption of **Fl** at 258 nm being replaced by one at 287 nm and two new transitions appearing in the visible region of the spectrum. This behaviour is generally similar to that which occurs on reduction of other aromatic molecules, for example the ligand-based reduction of $[Ru(bipy)_3]^{2+}$.[23]

Table 2 Electronic spectra of complexes **1** and **2** and their electrochemically-generated reduction products (CH_2Cl_2, 243 K)

	λ_{max}/nm (10^{-3} ε/dm^3 mol^{-1} cm^{-1})
1	517 (4.1), 363 (35), 322 (24), 297 (22), 260 (24)
[**1**]$^-$	1228 (1.7), 626 (4.6), 489 (9.6), 414 (27), 354 (26), 287 (24)
[**1**]$^{2-}$	1186 (20), 929 (24), 481 (25), 308 (22), 261 (20)
2	539 (8.1), 483 (10), 385 (63), 318 (42), 283 (33)
[**2**]$^-$	1319 (8.4), 1033 (13), 716 (12), 447 (49), 359 (33), 279 (32)
[**2**]$^{2-}$	1344 (74), 1142 (60), 593 (38), 549 (sh), 268 (30)
[**2**]$^{3-}$	1190 (80), 498 (38), 318 (22)

Because it is important to understand the spectral properties of **Fl**$^{\bullet -}$ before assignment of the spectra of the reduced forms of **1** and **2** can be made, we performed a ZINDO calculation on both **Fl** and **Fl**$^{\bullet -}$ to predict the electronic spectra. The results are in Table 1, together with the details of the measured spectra. For **Fl** there is a very good agreement between the positions of the calculated and actual peaks, although the predicted relative intensities of the two lower-energy peaks are inverted, with the 295 nm peak too weak and the 378 nm peak (predicted at 452 nm) too intense. For **Fl**$^{\bullet -}$ the agreement is again generally very good with an obvious correspondence between the predicted and actual peaks; the only problem again is the low predicted intensity of the *ca.* 290 nm peak and the somewhat high predicted intensity of the lowest energy transition (observed, 717 nm; predicted, 696 nm). The most important point is that the *ca.* 700 nm transition, not previously observed, is accounted for. Examination of the molecular orbitals of **Fl**$^{\bullet -}$ shows that the three frontier π-orbitals (HOMO, SOMO and LUMO) have energies of −3.87, −2.02 and +3.69 eV, suggesting that this lowest energy peak arises from a HOMO→SOMO transition.

UV/VIS/NIR spectroelectrochemical studies on complex 1

The electronic spectrum of **1** (Table 2, Fig. 5) shows the usual Mo(0)→pyridine MLCT transition at 517 nm.[4,7,17,18] The very intense transition at 363 nm we ascribe to a π→π* transition based on the ligand L^1; although the *ca.* 300 nm absorption peak of unsubstituted fluorenone is relatively weak (ε *ca.* 4000 dm^3 mol^{-1} cm^{-1}, Table 1), this becomes lower in energy and much more intense on addition of conjugated substituents to the fluorenone core.[24]

On one-electron reduction of **1** to [**1**]$^-$ (Fig. 5), the changes that occur are consistent with reduction of the fluorenone-based ligand. New transitions appear to the low-energy side of the original ligand-centred (363 nm) transition. In particular the new medium-intensity transition at 626 nm is the analogue of the characteristic **Fl**$^{\bullet -}$ transition at 535 nm (Fig. 4), but at lower energy because of the more extended conjugated system of L^1; likewise the relatively weak transition at 1228 nm

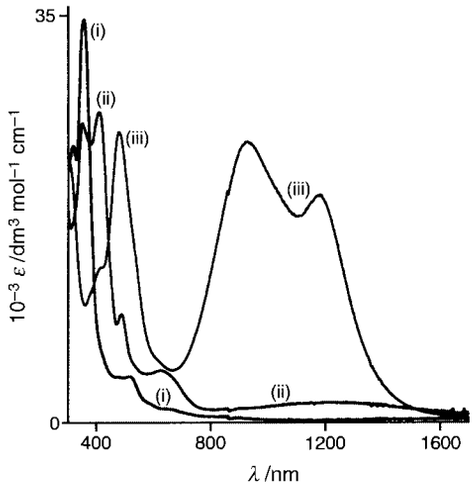

Fig. 5 Electronic spectra of (i) **1**, (ii) $[\mathbf{1}]^-$ and (iii) $[\mathbf{1}]^{2-}$ in CH_2Cl_2 at 243 K.

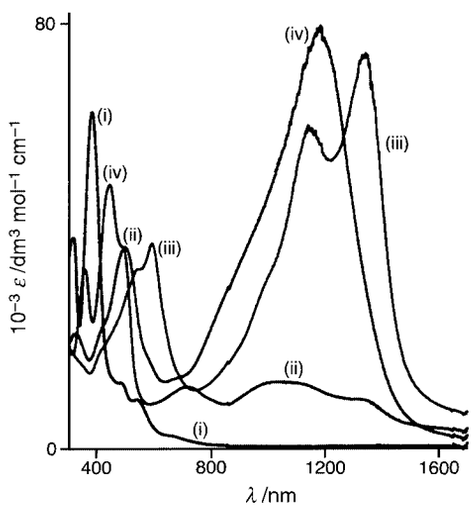

Fig. 6 Electronic spectra of (i) **2**, (ii) $[\mathbf{2}]^-$, (iii) $[\mathbf{2}]^{2-}$ and (iv) $[\mathbf{2}]^{3-}$ in CH_2Cl_2 at 243 K.

($\varepsilon = 1700$ dm^3 mol^{-1} cm^{-1}) is directly analogous to the 717 nm transition of $\mathbf{Fl}^{\bullet -}$, but again red-shifted for the same reason.

The second one-electron reduction to give $[\mathbf{1}]^{2-}$ results in the appearance of strong (ε *ca.* 20000 dm^3 mol^{-1} cm^{-1}) near-IR transitions at 929 nm and 1186 nm. This is entirely consistent with metal-centred reduction to give a Mo(0) centre, as described above, with these new transitions being Mo(0)→py MLCT in character.[4,7] Overall, the evolution of the electronic spectra of **1** during the two reductions clearly confirms the assignments that were made earlier on the basis of EPR spectroscopy, *viz.* that the first reduction is based on the fluorenone unit and the second is based on the metal.

UV/VIS/NIR spectroelectrochemical studies on complex 2

The electronic spectra of **2** and its reduction products up to $[\mathbf{2}]^{3-}$ are in Fig. 6 and Table 2. The extremely negative potential of the fourth reduction meant that it was not amenable to study by spectroelectrochemical methods, as there was evidence for slow decomposition of $[\mathbf{2}]^{4-}$ over the several-hour timescale of the experiment.

The spectrum of $[\mathbf{2}]^-$ is, like that of $[\mathbf{1}]^-$, consistent with the first reduction being localised on the fluorenone group. The principal π→π* transition of **2** at 385 nm is red-shifted to 447 nm, and a new transition of moderate intensity appears in the visible region (716 nm; *cf.* 626 nm for $[\mathbf{1}]^-$ and 535 nm for $\mathbf{Fl}^{\bullet -}$). In addition a new transition appears in the near-IR region which looks similar to the fluorenone-based HOMO→SOMO transition of $[\mathbf{1}]^-$, albeit of greater intensity, possibly due to a greater degree of vectorial charge transfer within the more extended ligand L^2. The contrast between the spectra of $[\mathbf{2}]^-$ and $[\mathbf{2}]^{2-}$ is obvious; the very strong new transition at 1344 nm ($\varepsilon = 74000$ dm^3 mol^{-1} cm^{-1}) is clearly analogous to the Mo(0)→py MLCT transitions that were observed in the reduced forms of the extended dinuclear complexes such as $[\{Mo(Tp^{Me,Me})(NO)Cl\}_2\{NC_5H_4(CH{=}CH)_nC_5H_4N\}]^-$ (*e.g.* for $n = 4$: $\lambda = 1282$ nm, $\varepsilon = 65000$ dm^3 mol^{-1} cm^{-1}).[4]

The site of the third reduction to $[\mathbf{2}]^{3-}$ is not obvious from the electronic spectrum, because the spectrum of $[\mathbf{2}]^{2-}$ contains so many very intense peaks that further changes are not as easy to see as the obvious changes which occurred on the first two reductions. However, with a bridging ligand of this length the potentials of the two Mo(0)/Mo(I) redox couples are not expected to be split by much,[4,17] whereas we would expect a much larger separation between two reductions localised on the fluorene units.[19] We therefore assign the third reduction to the remaining metal centre and the very negative fourth reduction to the bridging ligand, such that the sequence of the four reductions is ligand–metal(1)–metal(2)–ligand.

It is interesting to compare the separation of 240 mV between the two Mo(0)/Mo(I) couples of **2** (at −1.90 and −2.14 V *vs.* Fc/Fc^+) with the behaviour of complex **3**, in which the two Mo(0)/Mo(I) couples are essentially coincident because of a very weak interaction between them despite the similar length and conformation of the bridging ligand. Similarly, if the four-atom pathway across a *para*-substituted phenyl ring is counted as equivalent to two C=C units, then the bridging ligand L^2 is approximately equivalent in terms of length and degree of conjugation to the bridging ligand of $[\{Mo(Tp^{Me,Me})(NO)Cl\}_2\{NC_5H_4(CH{=}CH)_6C_5H_4N\}]$ in which (like **3**) the two Mo(0)/Mo(I) redox couples are again essentially coincident. It would be tempting to ascribe the 240 mV separation between the Mo(0)/Mo(I) redox couples of **2** to the presence of the extra electronegative (oxygen) atom in the bridging ligand, which could lower the energy of the π-orbitals responsible for the electronic interaction and make them more accessible, were it not for the fact that the initial ligand-centred reduction of L^2 will have the opposite effect.

Conclusions

We have used a combination of EPR and UV/VIS/NIR spectroelectrochemical methods to assign the combination of ligand-centred and metal-centred reductions which occurs in complexes containing a redox-active metal fragment [showing Mo(0)/Mo(I) and Mo(I)/Mo(II) couples] linked to a redox-active ligand (containing a fluorenone unit). In the dinuclear complex **2**, initial reduction of the bridging ligand is followed by two metal-centred reductions and finally the second ligand-centred reduction. The initial reduction of the bridging ligand results in a much larger separation between the two Mo(0)/Mo(I) couples than occurs in complexes where the bridging ligand is not redox-active.

Acknowledgements

We thank the European Commission for a TMR/Marie Curie fellowship to A. B., and the EPSRC for a project studentship to S. M. C.

References

1 J. A. McCleverty and M. D. Ward, *Acc. Chem. Res.*, 1998, **31**, 842.
2 V. A. Ung, S. M. Couchman, J. C. Jeffery, J. A. McCleverty, M. D. Ward, F. Totti and D. Gatteschi, *Inorg. Chem.*, 1999, **38**, 365.
3 N. C. Harden, E. R. Humphrey, J. C. Jeffery, S.-M. Lee, M. Marcaccio, J. A. McCleverty, L. H. Rees and M. D. Ward, *J. Chem. Soc., Dalton Trans.*, 1999, 2417.

4 S. L. W. McWhinnie, J. A. Thomas, T. A. Hamor, C. J. Jones, J. A. McCleverty, D. Collison, F. E. Mabbs, C. J. Harding, L. J. Yellowlees and M. G. Hutchings, *Inorg. Chem.*, 1996, **35**, 760.
5 M. D. Ward, *Chem. Soc. Rev.*, 1995, **24**, 121; M. D. Ward, *Chem. Ind.*, 1996, 568.
6 O. Kahn, *Molecular Magnetism*, VCH, New York, 1993; R. J. Bushby and J.-L. Paillaud, in *Introduction to Molecular Electronics*, eds. M. C. Petty, M. R. Bryce and D. Bloor, Edward Arnold, London, 1995, pp. 72–91.
7 Some representative recent examples: M. Brady, W. Weng, Y. Zhou, J. W. Seyler, A. J. Amoroso, A. M. Arif, M. Böhme, G. Frenking and J. A. Gladysz, *J. Am. Chem. Soc.*, 1997, **119**, 775; M. Guillemot, L. Toupet and C. Lapinte, *Organometallics*, 1998, **17**, 1928; E. Ishow, A. Gourdon, J.-P. Launay, C. Chiorboli and F. Scandola, *Inorg. Chem.*, 1999, **38**, 1504; A. Klein, V. Kasack, R. Reinhardt, T. Sixt, T. Scheiring, S. Zalis, J. Fiedler and W. Kaim, *J. Chem. Soc.*, *Dalton Trans.*, 1999, 575.
8 R. Kowallick, A. N. Jones, Z. R. Reeves, J. C. Jeffery, J. A. McCleverty and M. D. Ward, *New J. Chem.*, 1999, **23**, 915.
9 S.-M. Lee, M. Marcaccio, J. A. McCleverty and M. D. Ward, *Chem. Mater.*, 1998, **10**, 3272; A. M. Barthram, R. L. Cleary, R. Kowallick and M. D. Ward, *Chem. Commun.*, 1998, 2695.
10 R. J. Mortimer, *Chem. Soc. Rev.*, 1997, **26**, 147; R. J. Mortimer, *Electrochim. Acta*, 1999, **44**, 2971; J. Fabian, H. Nakazumi and M. Matsuoka, *Chem. Rev.*, 1992, **92**, 1197.
11 C. J. Jones, J. A. McCleverty, S. J. Reynolds and C. F. Smith, *Inorg. Synth.*, 1985, **23**, 4; S. Trofimenko, *Inorg. Chem.*, 1969, **8**, 2675; A. S. Drane and J. A. McCleverty, *Polyhedron*, 1983, **2**, 53.
12 S.-M. Lee, R. Kowallick, M. Marcaccio, J. A. McCleverty and M. D. Ward, *J. Chem. Soc.*, *Dalton Trans.*, 1998, 3443.
13 D. A. Fiedler, M. Koppenol and A. M. Bond, *J. Electrochem. Soc.*, 1995, **142**, 862.
14 M. C. Zerner, ZINDO version 4.0.2 in the CAChe system, Oxford Molecular, Oxford, 1998.
15 G. M. Sheldrick, SHELXS-97 and SHELXL-97, University of Göttingen, 1997.
16 G. M. Sheldrick, SADABS, A program for absorption correction with the Siemens SMART area-detector system, University of Göttingen, 1996.
17 A. J. Amoroso, A. M. W. Cargill Thompson, J. P. Maher, J. A. McCleverty and M. D. Ward, *Inorg. Chem.*, 1995, **34**, 4828; A. M. W. Cargill Thompson, J. A. McCleverty and M. D. Ward, *Inorg. Chim. Acta*, 1996, **250**, 29; A. M. W. Cargill Thompson, J. Hock, J. A. McCleverty and M. D. Ward, *Inorg. Chim. Acta*, 1997, **256**, 331.
18 A. Das, J. P. Maher, J. A. McCleverty, J. A. Navas Badiola and M. D. Ward, *J. Chem. Soc.*, *Dalton Trans.*, 1993, 681.
19 R. O. Loutfy, C. K. Hsiao, B. S. Ong and B. Keoshkerian, *Can. J. Chem.*, 1984, **62**, 1877.
20 A. Das, J. C. Jeffery, J. P. Maher, J. A. McCleverty, E. Schatz, M. D. Ward and G. Wollermann, *Inorg. Chem.*, 1993, **32**, 2145; E. R. Humphrey, V. A. Ung, J. P. Maher, J. A. McCleverty and M. D. Ward, *J. Organomet. Chem.*, 1999, **573**, 202.
21 A. Kuboyama, *Bull. Chem. Soc. Jpn.*, 1964, **37**, 1540.
22 N. Hirota and S. I. Weissman, *J. Am. Chem. Soc.*, 1964, **86**, 2538; H. V. Carter, B. J. McClelland and E. Warhurst, *Trans. Faraday Soc.*, 1960, **56**, 455.
23 G. A. Heath, L. J. Yellowlees and P. S. Braterman, *J. Chem. Soc.*, *Chem. Commun.*, 1981, 287.
24 J. Lewis, P. R. Raithby and W.-Y. Wong, *J. Organomet. Chem.*, 1998, **556**, 219.

Paper 9/07303E